

Stress induced grain boundaries in thin Co layer deposited on Au and Cu

Tomasz Zientarski¹ · Dariusz Chocyk²

Received: 21 June 2016 / Accepted: 12 September 2016 / Published online: 21 September 2016
© The Author(s) 2016. This article is published with open access at Springerlink.com

Abstract In this work, the structure and stress evolution in Co/Au and Co/Cu two-layer systems during deposition were studied. The growth of this system is evaluated by employing molecular dynamic simulations with potentials based on the embedded atom method theory. We used the kinematical scattering theory and the Ackland–Jones bond-angle method to the structural characterisation of deposited layers. In both systems, only compressive stress is observed during the deposition process and process relaxation of stress is visible. In Co/Au systems, creation of grains and grain boundaries is observed.

1 Introduction

The growth of thin metal layers of the material on different substrates may results in different changes in the stresses in these layers [1]. Stress changes in the deposited layers are often accompanied by structural changes. Additionally, the structural changes are one of the mechanisms that cause stress relaxation in the deposited layers. Understanding the relationship between changes of stress and structure is very important for the application of such systems. In one-layer systems, stress changes may be caused by reconstruction or formation of defects. For a variety of transition metals, such as Fe, Ni, or Co, the reconstruction process induces self-organised growth [2–4]. However, for metals such as

Ag and Au, growth leads to creating point dislocations [5, 6]. In multilayer systems, there exist more mechanisms that can change the stress [7].

Many multilayer systems were studied; among others Co/Cu and Co/Au alloys and multilayer thin films have been intensively studied [8–10]. Chado et al. [10] studied the deposition of small clusters of Co on gold surfaces with regular defects. They concluded that the lattice mismatch between Au and Co is strong enough to stress storage from the early stages of growth, and the Co lattice relaxes to its bulk value. Amir et al. [8] observed that addition of Ag surfactant in Cu/Co multilayers results in smoother and symmetrical interfaces and inhibits the interfacial alloying across the interfaces in Cu/Co multilayers. Without surfactant, they observed the metastable Cu/Co phases grow at the interfaces. Fu and coworkers used molecular dynamics simulation to study growth Pd/Cu and Cu/Pd [11]. They considered the influence of incident energy on the structure of two-layer systems. Their results showed that the surface roughness decreases with the increase in incident energy, and twin structures were also observed. Properties of thin films at the nano-scale level of thickness are still under intensive studies, motivated by the high importance of their application [12–14].

In the theoretical work, the molecular dynamics simulation method is commonly used, which includes the embedded atom method (EAM) applied to describe interactions [15–17]. This method allows an insight into the studied system at the atomic level, especially at the early stages of growth layers.

The aim of this work is to study change in the structure and stress of Co thin metal films deposited on Au and Cu substrate using three-dimensional molecular dynamics simulation. To investigate the development of the structure in Co films, the kinetic theory of scattering and Ackland–

✉ Tomasz Zientarski
t.zientarski@pollub.pl

¹ Institute of Computer Science, Lublin University of Technology, Nadbystrzycka 36B, 20-618 Lublin, Poland

² Department of Applied Physics, Lublin University of Technology, Nadbystrzycka 38, 20-618 Lublin, Poland

Jones method were applied. The stress is determined by the Basinski, Duesberry, and Taylor (BDT) atomic stress definition.

2 Simulation method

In this study, we applied the molecular dynamic simulations based on the method described in our work [18]. The process of deposition is simulated as a three-dimensional model as shown in Fig. 1. The rectangular simulation box has the dimensions $L_x \times L_y \times L_z$ ($48.96 \text{ \AA} \times 48.96 \text{ \AA} \times 40.00 \text{ \AA}$) for Au substrate and $L_x \times L_y \times L_z$ ($43.44 \text{ \AA} \times 43.44 \text{ \AA} \times 40.00 \text{ \AA}$) for Cu substrate. In both cases, the periodic boundary conditions were applied in x and y directions. The initial systems are composed of an unmovable substrate and several buffer layers of the same metal. These layers are assumed to be the (001) plane of FCC regular crystal with bulk crystal lattice constants equal to $a_{\text{Au}} = 4.08 \text{ \AA}$ and $a_{\text{Cu}} = 3.62 \text{ \AA}$. In contrast to the substrate, atoms in the buffer layers can change their position during simulation. Before the deposition process, buffer layer was equilibrated. Equilibration process minimises energy of system giving a stable configuration. Such configuration has no zero values of stress and depends on the temperature of the system. In this paper, we consider the systems at the same temperature. The time step was $\Delta t = 0.005 \text{ ps}$. Hereafter, the time is expressed as a number of the time steps. The deposition rate V of atoms is expressed as a ratio of the number of deposited atoms per number of time steps ($V = 1/2000$). The lower value of this ratio corresponds to the lower value of the real deposited rate. The temperature during the simulation was equal to 300 K , and the energy of deposition was always equal to 1 eV . The temperature during the simulation was kept fixed by periodical velocity rescaling. The deposited atoms and atoms in the buffer layer are under thermal

control. The atomic velocities of these layers are rescaled at every five-time steps. To prevent the atoms from leaving the simulation box, a reflecting wall was placed at its top. The simulation process was divided into two stages. At first, we created and deposited atoms. The particles were created at random (x, y) positions and initially oriented perpendicular to the bottom surface. Next, the system obtained was equilibrated by periodical velocity rescaling.

In our simulation, the interactions between metal atoms were described by the embedded atom method (EAM). In the EAM, the total energy E can be expressed as:

$$E = \sum_i F_i(\rho_i) + \frac{1}{2} \sum_{i,j(i \neq j)} \phi_{ij}(r_{ij}), \quad \rho_i = \sum_j f(r_{ij}) \quad (1)$$

where $F_i(\rho_i)$ is the embedding energy, $f(r_{ij})$ is the electron density function, ρ_i is the local electron density at site i , and ϕ_{ij} is the two-body potential between atoms i and j separated by distance r_{ij} . The embedding energy function is not dependent on the source of local electron density. Therefore, it can be used to calculate the energy in a pure and in a mixture system. The local electron density (ρ_i) at site i is a superposition of electron density of system atoms. The value of potential parameters [19] for Cu, Au, and Co is shown in Table 1.

For atomic system, the stress is determined by the position of atoms resulting from interatomic potential. The stress definitions include two parts. One part comes from

Table 1 EAM parameters [19]

	Cu	Au	Co
r_e	2.556162	2.885034	2.505979
f_e	1.554485	1.529021	1.975299
ρ_e	21.175871	19.991632	27.206789
ρ_s	21.175395	9.991509	27.206789
α	8.127620	9.516052	8.679625
β	4.334731	5.075228	4.629134
A	0.396620	0.229762	0.421378
B	0.548085	0.356666	0.640107
κ	0.308782	0.356570	0.5
λ	0.756515	0.748798	1.0
F_{n_0}	-2.170269	-2.937772	-2.541799
F_{n_1}	-0.263788	-0.500288	-0.219415
F_{n_2}	1.088878	1.601954	0.733381
F_{n_3}	-0.817603	-0.835530	-1.589003
F_0	-2.19	-2.98	-2.56
F_1	0.0	0.0	0
F_2	0.561830	1.706587	0.705845
F_3	-2.100595	-1.134778	-0.687140
η	0.310490	1.021095	0.694608
Fe	-2.186568	-2.978815	-2.559307

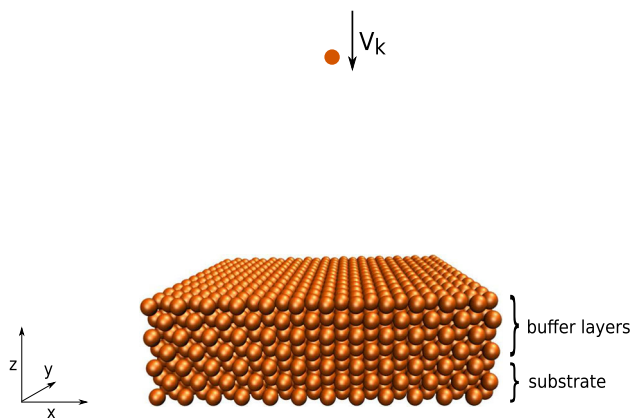


Fig. 1 Simulation model

the kinetic energy of the atoms, while the second part comes from interatomic forces. The atomic stress definition (BDT) was used [20]:

$$S_i = \frac{1}{V_i} \left[m_i v_i \otimes v_i + \frac{1}{2} \sum_{j \neq i}^N r_{ij} \otimes f_{ij} \right] \quad (2)$$

where m_i is the mass of the atom i , v_i is its velocity, $r_{ij} = r_i - r_j$ is the vector between atoms i and j , V_i is the volume of the atom i , f_{ij} is the interatomic force, N is the total number atoms in the domain, and \otimes denotes the tensor product of two vectors. In this work, the average stress S is defined as

$$S = \frac{1}{N} \sum_{i=1}^N S_i \quad (3)$$

where S_i represents the stress of the i -th atom, and N is the number of atoms in the deposited film. The stress is a tensor, whose diagonal elements S_{xx} , S_{yy} , and S_{zz} are stresses in the x , y , and z directions. The mean biaxial stress, S_{xy} , is expressed as $S_{xy} = (S_{xx} + S_{yy})/2$. The sign convention adopted here is such that the stress is positive for expansion and negative for compression.

In order to complete structure analyses of the simulation results, we applied the Ackland–Jones bond-angle method [21] and the kinematical scattering theory [22]. The Ackland–Jones bond-angle method allows us to determine the type of the crystalline structure of each atom. The X-ray diffraction technique is a powerful method widely used for the structural characterisation of real materials [23]. This technique was also been employed for interpreting the data obtained from simulation, in particular to establish the arrangement of atoms or to determine the lattice constant [24]. In order to calculate the X-ray scattering profiles, we applied the model based on the kinematical scattering theory proposed in [25] to calculate the X-ray scattering profiles. This model allows to calculate both specular and nonspecular X-ray scattering profiles in a wide range of scattering angles. The scattered X-ray intensity $I(\omega, 2\theta)$ can be calculated from the equation:

$$I(\omega, 2\theta) = \left| \sum_{i=1}^N \sum_{j=1}^M f_{i,j} \cdot \exp \left(-\frac{4\pi i}{\lambda_x} \cdot \sin \theta \cdot Z_{i,j}(\omega) \right) \right|^2 \quad (4)$$

where N is the number of in-plane simulated points, M is the number of atoms in the i -th column, λ_x is the X-ray wavelength, $f_{i,j}$ is the atomic scattering factor, $Z_{i,j}(\omega)$ is the distance of the considered (i, j) atom from the reference coordinate systems. The distance $Z_{i,j}(\omega)$ is calculated taking into account the fact that a sample is tilted from the specular position with a momentarily considered angle ω .

This model had earlier been applied to calculate the X-ray scattering profiles in Cu/Au and Fe/Au systems [18].

3 Results and discussion

We performed a series of molecular dynamic simulations of growing Co films on Au and Cu substrate. In each simulation, the total deposited film thickness was equal to ten monolayers, where one monolayer consists of 288 atoms. In Fig. 2, the evolution of the mean biaxial stress in deposited Co onto two different materials is presented. In both cases, changes in the stress are different. In the Co/Au system, a decrease in compressive stress is observed at the initial stage of growth. During the deposition process, the biaxial stress changes towards the tensile direction and gradually reaches a constant value that does not change until the end of the deposition process.

In the case of the Co/Cu system, stress changes are minor compared to the Co/Au system. At the initial stage of growth in the Co/Cu system, a small compressive value of stress is observed, next the deposited layers are relaxed for coverage up to one monolayer. Further growth results in a small compressive stress up to the end of the deposition. In Fig. 3, we present the dependence of stress components in x , y direction for Co/Au and Co/Cu. The shape of the stress component evolution for the deposited layers directly correlates with the total changes of stresses. Moreover, we did not observe any difference in stress components for cobalt atoms deposited on copper surfaces in contrast to those deposited on Au, in which the difference in stress components for coverage over 1500 deposited cobalt atoms is observed.

To analyse the arrangement of Co atoms deposited on Cu, we calculated the X-ray diffraction (XRD) intensity

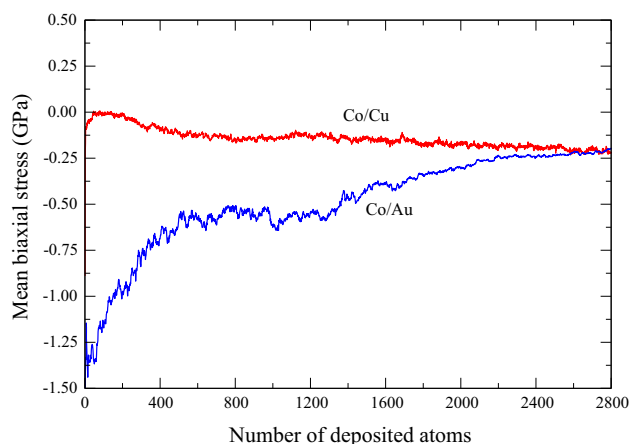


Fig. 2 Evolution of mean biaxial stress in the system (buffer layers + deposited atoms) during the deposition of Co on the Au and Cu substrate

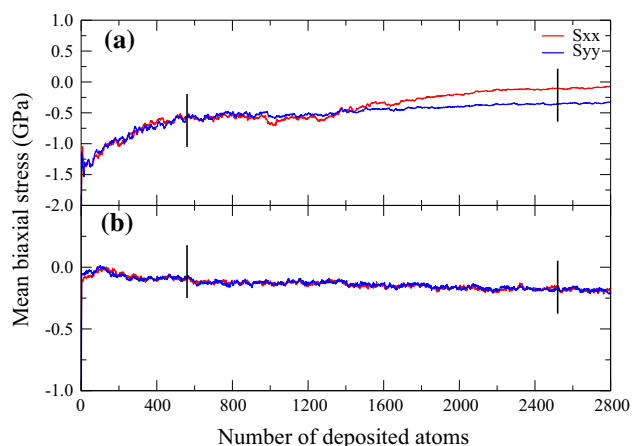


Fig. 3 Evolution of stress components in x and y directions in the system (buffer layers + deposited atoms) during the deposition process for the Co/Au (part **a**) and Co/Cu (part **b**) system

profiles. Figure 4 presents the XRD profiles obtained for Co atoms deposited on Cu were presented. The profiles were scanned in two perpendicular directions (x , y) for coverage corresponding to 500 and 2500 deposited atoms. The selected thickness of the deposited material corresponds to points before and after the separation of the stress components in the x and y directions presented in Fig. 3. The XRD profiles obtained for both directions show the presence of only one peak at an interplane distance equal to 1.81 Å. The observed peaks correspond to the distances that occur in the copper buffer layers. This result suggests that the deposited cobalt layers, despite significant differences in the lattice constant, fit the crystal lattice of Cu. Moreover, the intensity and position of XRD peaks in (x , y) direction are the same.

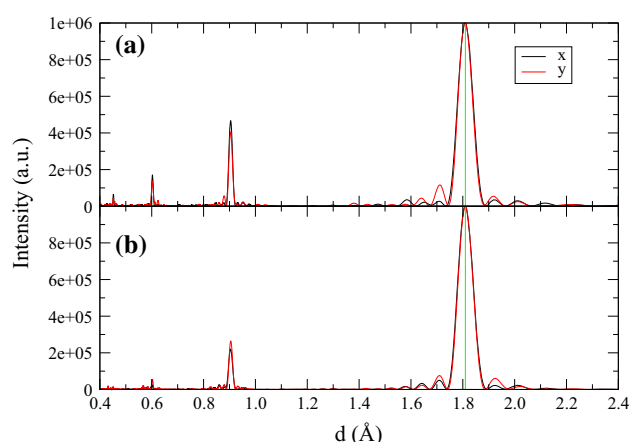


Fig. 4 XRD intensity profiles calculated in Co layers deposited on Cu. Intensities are scanned along x and y , and presented as dependences of interatomic distance. Intensity profiles are calculated for the amount of deposited cobalt atoms equal to 500 (part **a**) and 2500 (part **b**)

Similar calculations were performed for cobalt atoms in the Co/Au system. Figure 5 shows the results of XRD profiles for Co atoms deposited on Au. For coverage corresponding to 500 deposited cobalt atoms, we observed more than one peak in both directions scanned. For y direction, we observed two peaks, but for x more than twice. These results suggest that in deposited materials there exist different regions with different interplane distances. One can see that for higher coverage a better ordering of deposited atoms in both directions is observed. The position of the peak in y direction corresponds to a position of gold peaks and suggests that the Co lattice is partially matched to the Au lattice. In x direction, we observed two separated interplanar distances. These results suggest that in Co/Au systems there exists two different crystallographic structures.

The Ackland–Jones bond-angle method is used to the structural characterisation of crystal structures obtained from simulation data, e.g. FCC, BCC, and HCP assigned to atoms. In Figs. 6 and 7, we present examples of 3D configurations obtained from simulation at the end of the deposition process ($N = 2500$) for Co/Cu and Co/Au, respectively. The open Ovito [26] software was used to colour the atoms with different local structure.

From Fig. 6, it can be seen that the dominant ordering of the deposited Co layers are the FCC and BCC. The result obtained is consistent with the XRD profiles obtained for this system. XRD profiles for the FCC structure are insensitive to the presence of the BCC structure rotated by 45° and fitted to the FCC structure in the plane parallel to the substrate and give only one main peak. The deposited cobalt layer has ordered according to the FCC structure of the copper layer. The value of the stress is relatively small.

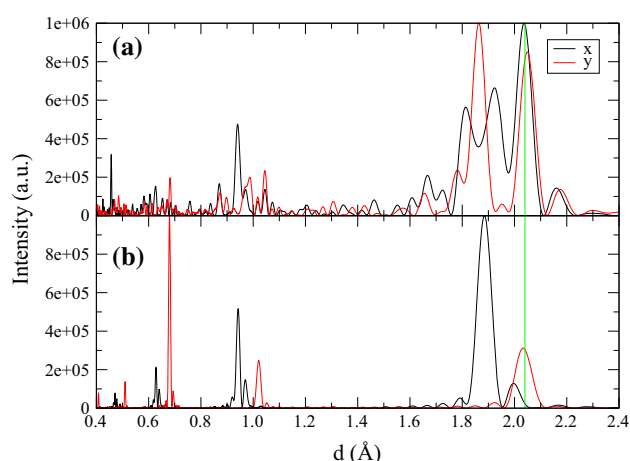


Fig. 5 XRD intensity profiles calculated in Co layers deposited on Au. Intensities are scanned along x and y , and presented as dependences of interatomic distance. Intensity profiles are calculated for the amount of deposited cobalt atoms equal to 500 (part **a**) and 2500 (part **b**)

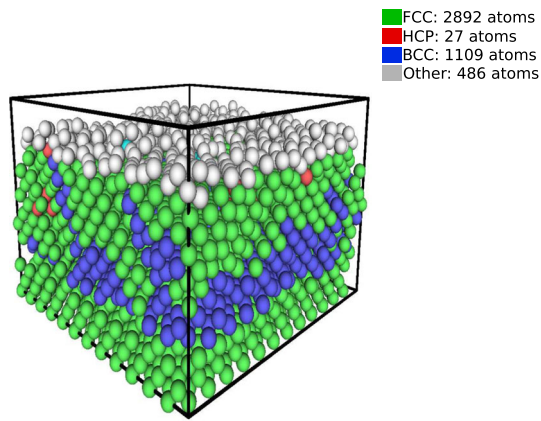


Fig. 6 3D configuration obtained from the simulation for the Co/Cu systems. The local lattice structure is indicated in colour (FCC—green, BCC—blue and HCP—red)

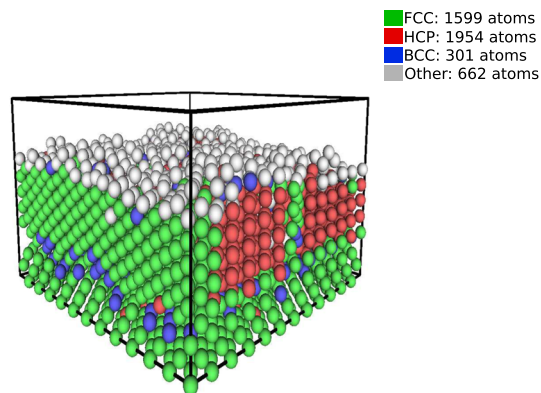


Fig. 7 3D configuration obtained from the simulation for the Co/Au systems. The local lattice structure is indicated in colour (FCC—green, BCC—blue and HCP—red)

Matching the structure of the deposited layer minimises stresses in the system and results in stress isotropy.

In contrast to Co/Cu systems, there is a large amount of the HCP structure in the Co/Au system, as shown in Fig. 7. We observe the grain structure and grain boundaries in one direction only. Atoms in grains have the HCP structure, but atoms in boundary regions have the FCC structure. The presence of two characteristic distances in x direction results in the two visible peaks in the XRD profiles. However, in y , the XRD profile shows the presence of one characteristic interatomic distance corresponding to the substrate layer. This result suggests adjustment of the HCP and FCC structures in y direction. Due to the differences in the crystallographic lattice structure of cobalt and gold, the expected stress should be large. Figure 2 shows that stresses gradually relax with an increasing amount of the deposited material. For an amount of deposited material corresponding to ≈ 1400 atoms, we observe a faster relaxation of the stress component S_{xx} . This process is

connected with the formation of grains (HCP) intersected by grain boundaries (FCC). Another factor resulting in the stress relaxation is tensile stresses generated by deposited Co atoms. The creation of grains in one direction causes the loss of coherence in this direction. This process allows a better fit of the crystalline lattice in the perpendicular direction. The stress changes in the Co/Au structure are mainly due to the relaxation in x direction.

4 Conclusions

The paper presents the results of the molecular dynamics simulation of the stress evolution during the deposition of Co films on Au and Cu surface.

The most important results from this study include the following:

- In both the Co/Au and Co/Cu systems at the early stage of growth, one observes compressive stress. Moreover, stress relaxation with increasing the thickness of the deposited materials is observed.
- In the Co/Cu systems, stress relaxation was observed due to the crystallisation of a mixture of cobalt and copper atoms forming an FCC and a rotating BCC structure. In this way, the system relaxes stresses.
- In the Co/Au case, relaxation occurs in a different way. Cobalt atoms are much smaller than gold atoms and initially crystallise together with the gold to form a mixture of grains with different crystallographic structures. With the increase in the number of cobalt atoms increases its impact on the surrounding atoms, and at a certain thickness grains (HCP) and grain boundaries (FCC) are created. This process relaxes stress.

Open Access This article is distributed under the terms of the Creative Commons Attribution 4.0 International License (<http://creativecommons.org/licenses/by/4.0/>), which permits unrestricted use, distribution, and reproduction in any medium, provided you give appropriate credit to the original author(s) and the source, provide a link to the Creative Commons license, and indicate if changes were made.

References

1. R. Koch, Stress in evaporated and sputtered thin films—a comparison. *Surf. Coat. Technol.* **204**, 1973–1982 (2010)
2. J.A. Strosio, D.T. Pierce, R.A. Dragoset, P.N. First, Microscopic aspects of the initial growth of metastable fcc iron on Au (111). *J. Vac. Sci. Technol. A* **10**, 1981–1985 (1992)
3. D.D. Chambliss, R.J. Wilson, S. Chiang, Nucleation of ordered Ni island arrays on Au (111) by surface-lattice dislocations. *Phys. Rev. Lett.* **66**, 1721–1724 (1991)
4. B. Voigtlander, G. Meyer, N.M. Amer, Epitaxial growth of thin magnetic cobalt films on Au (111) studied by scanning tunneling microscopy. *Phys. Rev. B* **44**, 10354–10357 (1991)

5. M.M. Dovek, C.A. Lang, J. Nogami, C.F. Quate, Epitaxial growth of Ag on Au (111) studied by scanning tunneling microscopy. *Phys. Rev. B* **40**, 11973–11975 (1989)
6. D.D. Chambliss, R.J. Wilson, S. Chiang, Ordered nucleation of Ni and Au islands on Au (111) studied by scanning tunneling microscopy. *J. Vac. Sci. Technol. B* **9**, 933–937 (1991)
7. Y.P. Li, G.P. Zhang, On plasticity and fracture of nanostructured Cu/X (X = Au, Cr) multilayers: the effects of length scale and interface/boundary. *Acta Mater.* **58**, 3877–3887 (2010)
8. S.M. Amir, M. Gupta, A. Gupta, Surfactant controlled interfacial alloying in thermally evaporated Cu/Co multilayers. *J. Alloys Compd.* **522**, 9–13 (2012)
9. T. Fu, X. Peng, S. Weng, Y. Zhao, F. Gao, L. Deng, Z. Wang, Molecular dynamics simulation of effects of twin interfaces on Cu/Ni multilayers. *Mater. Sci. Eng. A* **658**, 1–7 (2016)
10. I. Chado, C. Goyhenex, H. Bulou, J.P. Bucher, Evolution of the morphology of small Co clusters grown on Au(111). *Appl. Surf. Sci.* **226**, 178–184 (2004)
11. T. Fu, X. Peng, C. Feng, Y. Zhao, Z. Wang, MD simulation of growth of Pd on Cu (111) and Cu on Pd (111) substrates. *Appl. Surf. Sci.* **356**, 651–658 (2015)
12. E. Chason, A kinetic analysis of residual stress evolution in polycrystalline thin films. *Thin Solid Films* **526**, 1–14 (2012)
13. P.O. Renault, D. Faurie, E. Le Bourhis, G. Geandier, M. Drouet, D. Thiaudiere, Ph Goudeau, Deposition of ultra-thin gold film on in situ loaded polymeric substrate for compression tests. *Mater. Lett.* **73**, 99–102 (2012)
14. J. Zhang, Ch. Liu, Y. Shu, J. Fan, Growth and properties of Cu thin film deposited on Si(001) substrate: a molecular dynamics simulation study. *Appl. Surf. Sci.* **261**, 690–696 (2012)
15. M.S. Daw, M.I. Baskes, Embedded-atom method: derivation and application to impurities and other defects in metals. *Phys. Rev. B* **29**, 6443–6453 (1984)
16. S.M. Foiles, M.I. Baskes, M.S. Daw, Embedded-atom-method functions for the fcc metals Cu, Ag, Au, Ni, Pd, Pt, and their alloys. *Phys. Rev. B* **33**, 7983–7991 (1986)
17. Z.S. Pereira, E.Z. da Silva, Martensitic transformation of Cu on Ag(001) and Cu on Au(001) studied with classical molecular dynamics. *Phys. Rev. B* **79**, 115404–115411 (2009)
18. T. Zientarski, D. Chocyk, Structure and stress in Cu/Au and Fe/Au systems: a molecular dynamics study. *Thin Solid Films* **562**, 347–352 (2014)
19. X.W. Zhou, R.A. Johnson, H.N.G. Wadley, Misfit-energy-increasing dislocations in vapor-deposited CoFe/NiFe multilayers. *Phys. Rev. B* **69**(10), 144113 (2004)
20. Z.S. Basinski, M.S. Duesberry, R. Taylor, Influence of shear stress on screw dislocations in a model sodium lattice. *Can. J. Phys.* **49**, 2160–2180 (1971)
21. G.J. Ackland, A.P. Jones, Applications of local crystal structure measures in experiment and simulation. *Phys. Rev. B* **73**, 054104 (2006)
22. J.M. Cowley, *Diffraction Physics* (Elsevier, Amsterdam, 1995)
23. C.E. Bach, M. Giesen, H. Ibach, T.L. Einstein, Stress relief in reconstruction. *Phys. Rev. Lett.* **78**, 4225–4228 (1997)
24. T. Watanabe, K. Tatsumura, I. Ohdomari, *SiO₂/Si* interface structure and its formation studied by large-scale molecular dynamics simulation. *Appl. Surf. Sci.* **237**, 125–133 (2004)
25. D. Chocyk, A. Proszynski, G. Gładyszewski, S. Labat, P. Gergaud, O. Thomas, Determination of stress in Au/Ni multilayers by symmetric and asymmetric X-ray diffraction. *Opt. Appl.* **32**, 333–337 (2002)
26. A. Stukowski, Structure identification methods for atomistic simulations of crystalline materials. *Model. Simul. Mater. Sci. Eng.* **20**, 045021 (2012)